Terahertz time-domain study of a pseudo-simple-cubic photonic lattice

Takemitsu Aoki and Mitsuo Wada Takeda
Department of Physics, Faculty of Science, Shinshu University, Matsumoto 390-8621, Japan

Joseph W. Haus and Zhenyu Yuan
Electro-Optics Program, The University of Dayton, Dayton, Ohio 45469-0245

Masahiko Tani and Kiyomi Sakai
Kansai Advanced Research Center, Communication Research Laboratory, Iwaoka, Kobe 651-2401, Japan

Noriko Kawai and Kuon Inoue
Research Institute for Electronic Science, Hokkaido University, Kita-ku, Sapporo 060-0812, Japan
(Received 5 January 2001; published 29 June 2001)

A pseudo-simple-cubic photonic crystal lattice was fabricated in silicon. The phase-shift spectra and the amplitude spectra of the transmitted electromagnetic wave are studied by Terahertz time-domain spectroscopy measurements. The π phase shifts between Fabry-Perot modulation peaks are clearly observed. Our results are in good correspondence with transfer-matrix calculations. The dispersion curves were qualitatively extracted from the frequency dependence of the phase shifts. The gradient of the phase shift becomes large at the band-gap edges. This suggests that the group velocity is correspondingly small near the Brillouin-zone boundary.

DOI: 10.1103/PhysRevB.64.045106 PACS number(s): 71.15.Ap, 42.70.Qs, 42.25.Bs

I. INTRODUCTION

The possible suppression of spontaneous emission in periodic dielectric structures, also called photonic crystals, was first proposed in a paper by Yablonovich.[1] Further intense research on photonic crystals has subsequently uncovered interesting applications.[2] The techniques for calculating the dispersion in infinite structures are well developed. Calculations were published by Ohtaka,[3] but methods have subsequently been used by many groups to study the so-called photonic band structure; for a review of three-dimensional lattices see Ref. 4.

One motivation for recent investigations is to establish parameters for the existence of a photonic band gap, i.e., a frequency range where no propagating electromagnetic mode exists. This can be achieved by means of the proper choice of the lattice structure and the dielectric constants. This frequency region is called a photonic band gap (PBG). Since electromagnetic modes with frequencies in the absolute gaps are totally absent, spontaneous emission is forbidden in situations where the band gap overlaps the electronic band edge. The inhibition of spontaneous emission can improve the performance of many optoelectronic devices such as semiconductor lasers with high efficiency. For these purposes, development of a lattice with the gap frequency at visible and near-infrared region is inevitably important. However, those lattices are technically very difficult to fabricate at present.

In this connection, one of the authors has coproposed a simple cubic (SC) structure exhibiting a full PBG.[5] A modified geometry using the SC symmetry may be possible to fabricate by molecular-beam epitaxy and lithography techniques. Recently, Wada *et al.*[7] reported a comparison of the transmission spectrum profiles between results of theoretical matrix transfer technique calculations[6] and Fourier transform infrared (FTIR) experimental observations of a pseudo-simple-cubic lattice composed of air rods with square- and circular-shaped rods made of silicon. The lattice constant of that sample was 0.53 mm.[7] In that paper, we speculated that samples four to eight periods thick would be sufficient for suppressing spontaneous emission because the transmission in the band-gap region was reduced by a factor of more than 100.

In our earlier FTIR studies[7,8] the transmission amplitude spectra are not sufficient to understand the dispersion spectra, because the information about the phase of the waves is lost. Amplitude information is sufficient for identifying the band gaps and together with band-structure computations it can identify the origin of the total reflection, e.g., a true band gap or an uncoupled mode. However, to find the band dispersion we need the phase of the electromagnetic wave. This information is provided by time domain spectroscopy, which was previously used for two-dimensional photonic crystal studies.[9] Once the dispersion curves are found, they provide and estimate the group velocity.

In the following sections, the experimental setup and the data analysis are described. The sample geometry and material parameters are used in our simulations of the dispersion spectra and of the transmission spectra. Details about the sample size features in the data and the polarization dependence are examined.

II. EXPERIMENTAL DETAILS

For the present paper, a photonic crystal was fabricated in silicon. The sample symmetry was a distorted simple-cubic lattice that we call a pseudo-simple-cubic lattice. It is composed of square air rods with one bevel plane. The photonic band structure was determined by THz time-domain spec-

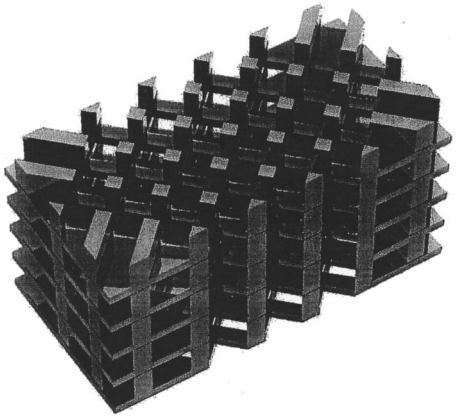

FIG. 1. Schematic of a pseudo-simple-cubic lattice composed of parallel square air rod in silicon. The top and bottom of the sample are perpendicular to the $\Gamma-Z$ direction and the sides are perpendicular to the $\Gamma-M$ direction.

troscopy (THz-TDS) measurements. It provides the complete information about the wave: the phase-shift spectra, as well as the amplitude spectra. From the frequency dependence of the phase shift, the dispersion curves of electromagnetic wave in the photonic crystal were qualitatively obtained.

A photonic crystal of pseudo-simple-cubic lattice composed of square air rods was fabricated in silicon. The schematic of the specimen is illustrated in Fig. 1; it was constructed by the following process. First, using a 0.40-mm-thick Silicon flat (100) plate, square cone holes were made through a plate using a wet-etch method; 169 holes were made in a 13×13 pattern with a lattice constant of 0.40 mm. Then, 13 parallel grooves, whose depth and width are 0.29 mm, were cut into the opposite side of plate with a numerically controlled diamond saw. The center-to-center distance between adjacent grooves is also 0.40 mm. Grooves along the indicated x and y directions also intersect over the holes etched in the z direction.

The air rods along the z axis are not simple square rods because they are partially replaced by square cone. The plate was cut into a rectanglular shape with 4.20×8.20 mm^2; its faces make an angle of $\pi/4$ with respect to the x and y axes. Ten identical plates were machined and holes were aligned with the aid of an optical microscope. The plates were stacked and fixed into the position with varnish. The specimen was constructed with (001), (110) and (-110) crystal plane, where along the $\langle001\rangle$ direction, i.e., z axis there are ten unit cells whereas along the $\langle110\rangle$ direction there are eight unit cells, which enable us to measure the transmission spectra both along $\Gamma-M$ ($\langle110\rangle$) as well as $\Gamma-Z$ ($\langle001\rangle$) directions.

As previously mentioned, the specimen is a quasi-simple-cubic lattice because the specimen mixed the square air rods of 0.29 mm edges along the x and y axes (see Fig. 1), with the square rods partially replaced by square cones perpendicular to them. The air volume filling factor is approximately 0.82. The dielectric constant is 11.4 in the frequency region of our experiments.

The field amplitude after passing through the photonic crystal is measured by a sampling technique. The detail of the experimental setup for generation and detection of THz radiation is shown in Ref. 10. A mode-locked Ti:sapphire laser pumped by a cw-Ar ion laser produces 80-fs full width at half maximum (FWHM) light pulses at a wavelength of ~780 nm and a repetition rate of 82 MHz. The femtosecond pump pulses are focused by an objective lens on the biased gap of the photoconductive antenna fabricated on a low temperature grown GaAs substrate.

The emitted THz radiation is collimated and focused by a pair of off-axis paraboloidal mirrors with a focal length of 150 mm and an effective diameter of 30 mm ($F=5.0$) onto our photonic crystal specimen. The transmitted radiation is collected and focused by another pair of off-axis paraboloidal mirrors with the same focal length and diameter onto a photoconductive sampling detector, which is also designed as a photoconductive antenna. Therefore, the incident and transmitted radiation approximate a plane wave at the sample position. The photoconductive detector is gated by a focused femtosecond probe beam pulses that are extracted from the pumped laser by a beam splitter. The wave form for the THz pulse is obtained by using an optical delay line to offset the overlap of the probe pulse with the THz signal. The dc photocurrent is driven by the THz field after the probe pulse induces carriers in the antenna; it is measured by an ammeter. The optical setup for THz radiation is placed in an evacuated box to reduce absorption by water vapor.

III. ANALYSIS AND DISCUSSION

The transmission spectra propagating along both $\Gamma-Z$ and $\Gamma-M$ directions and for orthogonal polarizations are found by Fourier transforming the THz-TDS data. The complex transmission function of the dielectric array is obtained by dividing the complex Fourier transform of the wave form with the specimen in place by the complex Fourier transform of the reference wave form without a specimen. The transmission function contains both amplitude and phase information, and represents the electromagnetic propagation properties of the photonic crystal. The phase of the detected signal with the specimen was subtracted from the phase of the signal without the specimen. The result is the net phase difference between the phase of the electromagnetic wave propagating through the photonic crystal and that propagating in the free space.

A common band gap was observed in both the $\Gamma-Z$ and $\Gamma-M$ directions around 10 cm^{-1}. In Fig. 2(a), the solid line shows the transmission intensity spectrum for $\Gamma-Z$ direction. It should be noted that the opaque region exists from 6.5 cm^{-1} to 10.2 cm^{-1}, which corresponds to the photonic band gap between the first band and the second band shown in Fig. 3. The band structure is calculated by a plane-wave expansion method with 729 plane waves. Uncoupled modes occur when the symmetry of the eigenmode in the crystal is incompatible with the symmetry of the incident wave;[11,12] uncoupled modes are assigned by symmetry as shown in Fig. 3. The transmission depends on the band symmetry and the polarization of the incident radiation. The transmission region below 6.5 cm^{-1} corresponds to the first band and that from 10.2 cm^{-1} to 15.9 cm^{-1} corresponds to the second

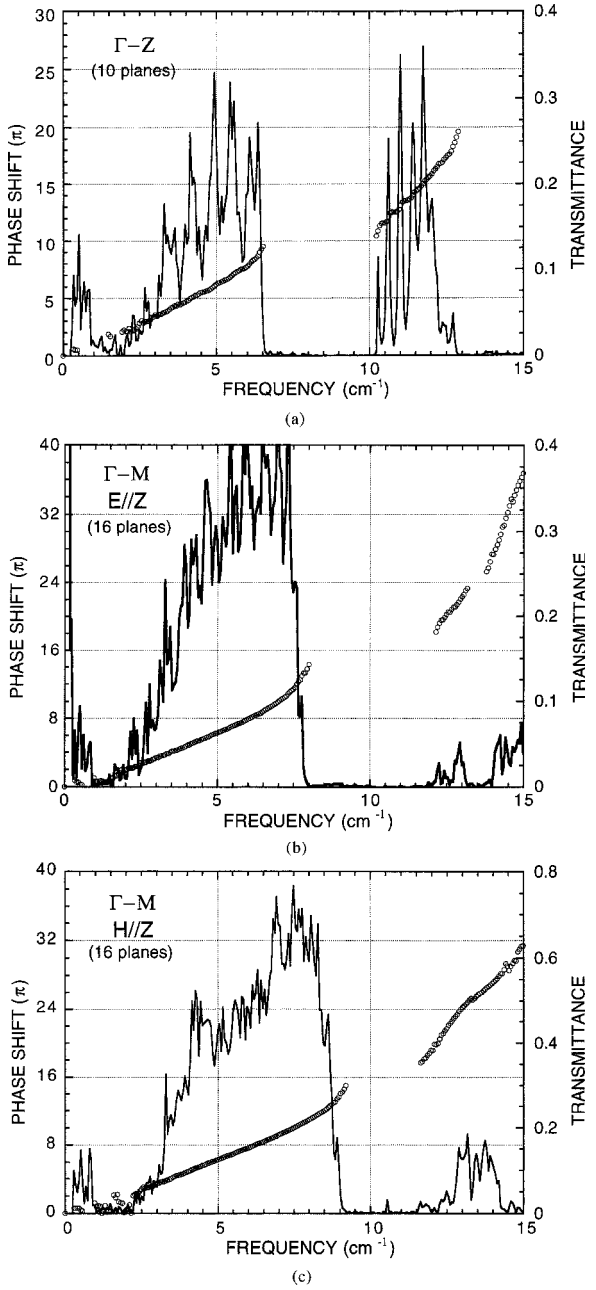

FIG. 2. Transmission intensity and phase-shift spectra of the pseudo-simple-cubic photonic crystal measured by THz time domain spectroscopy. (a) observed along the $\Gamma-Z$ direction (belongs to the E representation), (b) along $\Gamma-M$ with $E\|Z$ (B_1), and (c) along $\Gamma-M$ with $H\|Z$ (B_2).

band. The periodic or modulated transmittance features in both regions are due to the Fabry-Perot interference effects, which are thoroughly discussed below.

The open circles in Fig. 2(a) shows the net phase-shift spectrum for $\Gamma-Z$ direction. The row data of phase shift include an ambiguity of $n\pi$ radians. The phase of the second band region above 10.2 cm^{-1} has an additional π radian shift, because the phase slips by π across the band gap, as mentioned in the following section. In Figs. 2(b) and 2(c), the transmission intensities and net phase shifts measured along $\Gamma-M$ direction with E parallel to Z and H parallel to

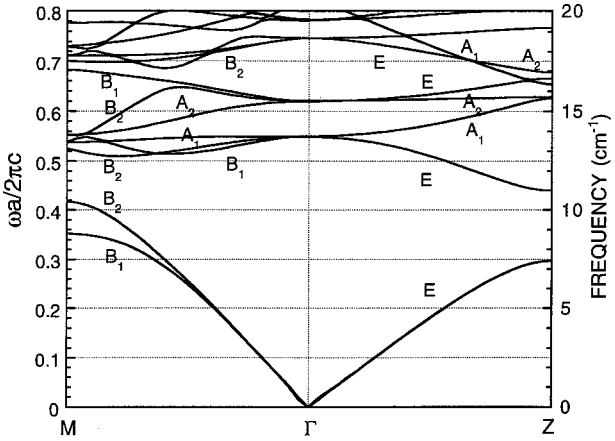

FIG. 3. Photonic band structure of the pseudo-simple-cubic lattice composed of parallel square air rods in silicon. The following parameters were assumed: the lattice constant is 0.40 mm, the cross section of the rod is 0.29×0.29 mm^2, and the dielectric constant of silicon is 11.4. The bands are labeled by the assignment of the symmetry of the band's eigenfunctions. The bands B_1, B_2, and E can couple to external plane-wave radiation. The E band is doubly degenerate. The modes labeled A_1 and A_2 are incompatible with the symmetry of the incident plane wave.

Z are shown, respectively. The band gaps are open between 7.8–11.8 cm^{-1} and 9.1–11.5 cm^{-1}, respectively. A sharp peak at 10.5 cm^{-1} is seen for the H-polarization in the $\Gamma-M$ transmission data. The origin of this peak may be due to a localized defect-mode due to imperfections in the lattice. The common band gap along $\Gamma-Z$ and $\Gamma-M$ is open between 9.1–10.5 cm^{-1}.

We have calculated the transmittance spectra for the lattice of the present structure with the same parameters, except the number of layers, by using the transfer-matrix method. For our purposes, we used a computer program developed by Pendry's group.[6] The simulation result for propagation along the z axis ($\Gamma-Z$ direction) with an eight-period-thick crystal is presented in Fig. 4. In the calculations, the lateral direction is infinite. The solid circles correspond to the intensity spec-

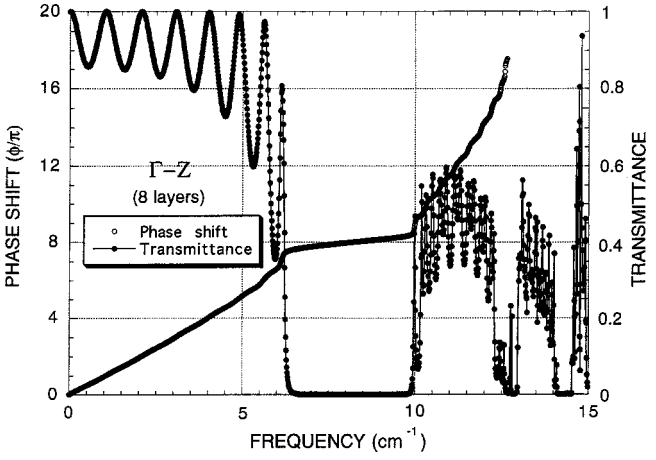

FIG. 4. Transmittance spectra of the pseudo-simple-cubic photonic crystal calculated by the transfer-matrix method along the $\Gamma-Z$ direction with the sample that is eight periods thick.

tra of transmittance and the open circles correspond to the phase-shift spectra. In the following sections, we will discuss the following aspects of the spectra: (A) Fabry-Perot interference, (B) photonic band gap, and (C) dispersion relation for the $\Gamma - Z$ direction.

A. Fabry-Perot interference

The transmission intensity shows maxima at frequencies corresponding to the standing waves in the specimen (Fabry-Perot effect); it is due to the interference between the electromagnetic wave reflected by the front and back surfaces of specimen. By analogy to standing waves in a one-dimensional periodic sample, the phase difference between the neighboring maxima should be π. This feature is seen in both observed and calculated spectra shown in Figs. 2 and 4. The influence of the interference is also observed in the spectrum of the phase shift (Fig. 4). That is, the phase shift remains almost constant in the region with low-transmission coefficient.

These wavelike vibrations are observed in the transmission amplitude spectra where high transmittance is measured, that is, in the region below 6.5 cm^{-1} and 10.2–15.9 cm^{-1} [Fig. 2(a)]. The number of transmission peaks corresponds to standing waves along the propagation direction in the photonic crystal. The phase change between each standing wave is π and at the Brillouin-zone boundary, the phase change $m\pi$ corresponds to one standing wave for each crystal plane, so when the frequency is changed from the center to the edge of the zone along a particular direction, the standing waves lead to transmission maxima. Thus, the number of transmission maxima in the frequency region to each branch corresponds to the number of crystal planes across the sample in the chosen propagation direction. For instance, in $\Gamma - Z$ direction, the number of unit cells (crystal planes) is ten, so that ten maxima should be counted for each frequency region corresponding to each branch. For the first branch (dielectric band) below 6.5 cm^{-1}, only six peaks are seen because of the low-signal intensity throughout the region below 3 cm^{-1}. However, using the average width between maximum peaks, which is about 0.7 cm^{-1}, we infer that the other four peaks must exist in the frequency region below 3 cm^{-1}, including a peak at 0 cm^{-1}. Thus, we expect ten maxima in the region corresponding to the first branch. In the region from 10.2 cm^{-1} to 13.0 cm^{-1}, corresponding to the second branch (air band), the identification is more difficult. However, we can observe eight peaks and one shoulder in Fig. 2(a). The flatter dispersion curve for this branch compresses the Fabry-Perot resonances into a smaller frequency range. The phase changes denoted by the open circles in Fig. 2(a) change by 10π in each band.

In the case of the $\Gamma - M$ direction, the specimen has eight unit cells, that is, there exist 16 (110) crystal planes along the $\Gamma - M$ direction. The phase should change by 16π in the first band. The open circles in Figs. 2(b) and 2(c) show the phase shift and they change about 16π until the center of the first band gap.

B. Photonic Band Gap

The opaque region of 6.5–10.2 cm^{-1} observed in transmission intensity spectrum for the $\Gamma - Z$ direction corresponds to the first band gap. From the direct analysis of the phase shift by THz time-domain spectroscopy, we cannot unambiguously determine the change of phase between the first and second branches. However, we can infer from analogy to the electronic band structure of semiconductors, in which the conduction band and the valence band surround the fundamental gap. The gap between the first and second bands occurs at the Brillouin-zone boundary at $k = \pi/a$. The modes are standing waves with a wavelength of $2a$, twice that of the lattice constant for $k = \pi/a$. Close to the band-gap edges, the standing waves are localized in different dielectric materials.

Near one band edge, the field maxima are located at the center of the high-ϵ (i.e., high-dielectric constant) layer, and near the other edge, it is located at the center of low-ϵ layer. By the electromagnetic variational theorem, the low-frequency modes concentrate their energy in the high-ϵ region (dielectric band), whereas the high-frequency modes concentrate their energy in the low-ϵ regions (air band). Therefore, the difference between the phase of mode at top of the first branch (dielectric band) and that at bottom of the second branch (air band) must be π. It is clearly identified by the simulation results in Fig. 4 that the phase shifts by π when tuning through the first band gap.

C. Dispersion relation

The open circles in Fig. 4 show the phase-shift spectra. The phase shift increases rapidly in the vicinity of maxima of transmission intensity and relatively slow around the minima as is shown in the phase-shift spectra both observed and calculated. This fact indicates that the optical density of state (ODOS) is very large around the frequency of each standing wave. Moreover, it should be noted that in the vicinity of band-gap edges, the ODOS must be very large.[13] The effective refractive index of the sample n_{eff} is deduced from the wave-number k by the expression $n_{eff} = \lambda k/2\pi$, where λ is the free space wavelength. The relationship between net phase-shift ϕ extracted from the experimental data and the wave number is obtained from

$$k(\omega) = \phi(\omega)/L, \tag{1}$$

where L is the thickness of the specimen.

As discussed in the Fabry-Perot section, the phase shift changes by $m\pi$ if there exist m crystal planes along the direction of the incident wave. The thickness of the specimen is ma, so that at the zone boundary, the phase should be $m\pi$. In the present specimen, the number of crystal planes along $\Gamma - Z$ and $\Gamma - M$ are 10 and 16, respectively. In Fig. 5 the zone boundary (Z) along $\Gamma - Z$ corresponds to 10π and that (M) along $\Gamma - M$ to 16π. The frequency dependence of the phase shift observed shows good correspondence with the dispersion curves estimated by the plane-wave expansion method (Fig. 3) along the $\Gamma - Z$ direction both qualitatively and quantitatively (E-modes).

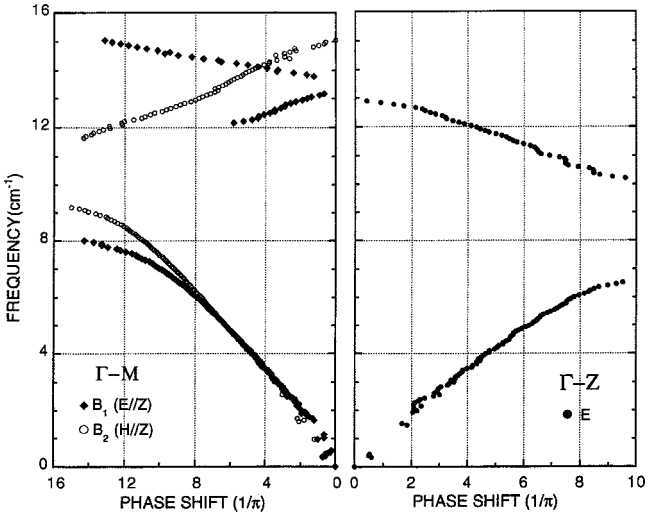

FIG. 5. Dispersion relation of the electromagnetic wave along $\Gamma-Z$ and $\Gamma-M$ direction in the pseudo-simple-cubic photonic crystal. The solid circles, solid diamonds, and open circles are estimated from the phase shift observed, and belong to the E, B_1, and B_2 irreducible representations, respectively.

Along the $\Gamma-M$, the frequencies of the second band observed both of B_1 and B_2 modes are somewhat higher than the calculated values. This discrepancy is attributed to the small number (729) of plane waves used in the plane-wave expansion method, where the convergence is insufficient. It should be noted that the gradient of the phase shift becomes very large at the band-gap edges. That is, the gradient of the dispersion curves is almost zero at the Brillouin-zone boundary. This indicates that the group velocity of the electromagnetic waves must become very small at the zone boundary.

IV. CONCLUSIONS

A pseudo-simple-cubic photonic crystal fabricated in silicon was interrogated by THz-TDS. The detailed transmission spectra results show a common gap for both polarizations in two different directions. The phase spectra agree in magnitude and shape with corresponding theoretical expectations. We also identified specific features of the Fabry-Perot resonances in the amplitude and phase data. The detailed analysis was in good agreement with expected results. The polarization dependence of the dispersion and the magnitude of the dispersion are in good agreement with plane-wave calculations. A full band gap is expected based on the plane-wave calculations and the results for specific propagation directions and polarizations are in good agreement with the calculations. This wide bandwidth spectroscopy provides a detailed account of the electromagnetic properties of finite photonic crystals.

ACKNOWLEDGMENTS

The authors are grateful to the SONIC-MILL Japan Corporation for kindly machining the sample. The authors express their sincere thanks to Professor K. Sakoda of Hokkaido University, and Professor K. Ohtaka and Dr. T. Ueta of Chiba University for helpful discussions. Thanks are also due to Professor J.B. Pendry for kindly providing the transfer-matrix program. This work was partly supported by a Grant of Aid for Scientific Research of Priority Areas, ''Photonic Crystal,'' and by that for General Scientific Research from the Ministry of Education, Science, Sport and Culture of Japan. This work was also partly supported by a Grant of Aid from Research Foundation for Opto-Science and Technology. JWH was supported by the National Science Foundation through Grant Nos. INT-9513137 and ECS-9630068.

[1] E. Yablonovich, Phys. Rev. Lett. **58**, 2059 (1987).
[2] Special review issues on photonic band-gap structures are: C.W. Bowden, J.P. Dowling, and H.O. Everitt, J. Opt. Soc. Am. B **10**, 280 (1993); G. Kurizki and J.W. Haus, J. Mod. Opt. 41 (1994).
[3] K. Ohtaka, Phys. Rev. B **19**, 5057 (1979).
[4] J.W. Haus, J. Mod. Opt. **41**, 195 (1994).
[5] H.S. Sozuer and J.W. Haus, J. Opt. Soc. Am. B **10**, 296 (1993).
[6] J.B. Pendry, J. Mod. Opt. **41**, 208 (1994).
[7] M. Wada, Y. Doi, K. Inoue, J.W. Haus, and Z. Yuan, Appl. Phys. Lett. **70**, 2966 (1997).
[8] M. Wada, Y. Doi, K. Inoue, and J.W. Haus, Phys. Rev. B **55**, 10 443 (1997).
[9] W.H. Robertson, G. Arjavalingham, R.D. Meade, K.D. Brommer, A.M. Rappe, and J.D. Joannopoulos, J. Opt. Soc. Am. B **10**, 322 (1993).
[10] M. Tani, S. Matsuura, K. Sakai, and S. Nakashima, Appl. Opt. **36**, 7853 (1997).
[11] K. Sakoda, Phys. Rev. B **51**, 4672 (1995); **55**, 15 345 (1997), and references therein.
[12] Z. Yuan, J.W. Haus, and K. Sakoda, Opt. Express **3**, 19 (1998).
[13] K. Ohtaka, Y. Suda, S. Nagano, T. Ueta, A. Imada, T. Koda, J. Bae, K. Mizuno, S. Yano, and Y. Segawa, Phys. Rev. B **61**, 5267 (2000).